JACS
JOURNAL OF THE AMERICAN CHEMICAL SOCIETY

Communication

pubs.acs.org/JACS

Optical Nanoimaging for Block Copolymer Self-Assembly

Jie Yan,[†,§] Ling-Xi Zhao,[†,§] Chong Li,[†,§] Zhe Hu,[†] Guo-Feng Zhang,[†] Ze-Qiang Chen,[†] Tao Chen,[†] Zhen-Li Huang,[†] Jintao Zhu,[‡] and Ming-Qiang Zhu*[,†]

[†]Wuhan National Laboratory for Optoelectronics and [‡]College of Chemistry and Chemical Engineering, Huazhong University of Science and Technology, Wuhan, Hubei 430074, China

Supporting Information

ABSTRACT: One approach toward optical nanoimaging involves sequential molecular localization of photoswitchable fluorophores to achieve high resolution beyond optical limit of diffraction. Block copolymer micelles assembled from polystryrene-*block*-poly(ethylene oxide) block copolymers (PSt-*b*-PEO) are visualized in optical nanoimaging by staining the polystyrene blocks with spiropyrans (SPs). SPs localized in hydrophobic phase of block copolymer micelles exhibit reversible fluorescence on−off switching at alternating irradiation of UV and visible light. Phase-selective distribution of SPs in block copolymer micelles enables optical nanoimaging of microphase structures of block copolymer self-assembly at 50-nm resolution. To date, this is the sturdiest realization of optical nanoimaging with subdiffraction resolution for solution self-assembly of block copolymers.

The self-assembly of block copolymers into well-defined micelles or nano-objects becomes an innovative technology in areas such as nanoscale materials,[1,2] high-resolution nanolithography,[3,4] and drug delivery.[5,6] Compared to small molecular surfactants and phospholipids, block copolymers offer superior flexibility in controlling micellar structure and functionality through the choices of polymer molecular weight, chemical contents, and molecular architecture.[7] It is of high practical significance to enable the nanoscale imaging of microphase structures from block copolymer self-assembly in a precise and facile fashion. The goal of visualizing the nanoscopic domains has stimulated numerous investigations on imaging methods including scanning electronic microscopy (SEM), transmission electronic microscopy (TEM), atomic force microscopy (AFM), and scanning tunnel microscopy (STM).[8−11] However, these methods are either invasive, high-vacuum, or time-consuming so that their application in real-time cellular biology, and in situ nondestructive detection is limited.[12] Fluorescence microscopy is extensively utilized for noninvasive, real-time bioimaging because one can observe in situ specific components through molecule labeling and living cellular events in real time.[13] However, the diffraction of light limits the spatial resolution of conventional fluorescence microscopy with about 200−300 nm in the lateral direction and 500−700 nm in the axial direction.[14] The spatial resolution scale in conventional fluorescence microscopy is comparable to or larger than general subcellular organelles but still unresolvable in subwavelength structures. In the past decades, some super-resolution fluorescence microscopy techniques have been developed to exceed the diffraction barrier, including techniques that exploit nonlinear effects to sharpen the point-spread function of the microscope, such as stimulated emission depletion (STED) microscopy[15−17] and the sequential localization of individual fluorescent molecules, such as stochastic optical reconstruction microscopy (STORM)[18−21] and photoactivated localization microscopy (PALM).[22,23] These methods have achieved an order of magnitude of enhancement in cellular spatial resolution in all three dimensions over conventional fluorescence microscopy. The spatial resolution for cellular imaging is enhanced down to tens of nanometers.

In conventional fluorescence imaging, the bright, steadfast probes are desirable to achieve strongest fluorescent signals. However, super-resolution imaging, here we term optical nanoimaging, depends on the ability of reversible switching of fluorophores between bright, emissive states and dark, non-emissive states or dual color emissive states.[24] Precious development of high-performance photoswitchable fluorophores and polymers enables their applications in all-optical transistor or super-resolution imaging.[25−27]

In spite of numerous reports on super-resolution imaging in cell biology,[18−23] the optical nanoimaging in material science such as inorganic nanomaterials, organic polymer self-assembly, and organic−inorganic composites has not yet been intensively explored.[28] As a proof-of-concept, here we develop an optical nanoimaging method utilizing a photoswitchable fluorophore, 2-(3′,3′-dimethyl-6-nitro-spiro[chromene-2,2′-indolin]-1′-yl) ethyl p-toluene sulfonate (SPTS) to stain the specific domains in microphase structures of block copolymer self-assembly in aqueous solution, which is shown in Scheme 1. Generally, most fluorophores used in STORM need the presence of cofactors like thiols, sodium boron hydride, pH, etc. and are usually accomplished in aqueous medium for cellular imaging.[29] The fluorophores based on spiropyrans (SPs) for nanoimaging are only sensitive to light irradiation (Scheme 1a) without any necessity of alien cofactors and hence have an expansive application. SPs display only photochromism in an aqueous medium, but without robust fluorescence and fluorescence switching.[25a] Thus, super-resolution imaging was not feasible in aqueous environment. However, in the hydrophobic solid microphase of block copolymer, SPs exhibit robust fluorescence switching, which is the key for optical nanoimaging. Thus, fluorescence switching of SPs is enabled by integrating SPs as staining agents into hydrophobic solid environment.[27a] Herein,

Received: November 28, 2014
Published: February 10, 2015

DOI: 10.1021/ja512189a
J. Am. Chem. Soc. 2015, 137, 2436−2439

Scheme 1. Principle of Optical Nanoimaging. (a) Schematic of Spiropyrans (SPs) and Merocyanine (MC) Transformation. (b) Schematic of Optical Nanoimaging for Microphase Structures of Block Copolymer Self-Assembly (Here Cylindrical Micelles and Vesicles)

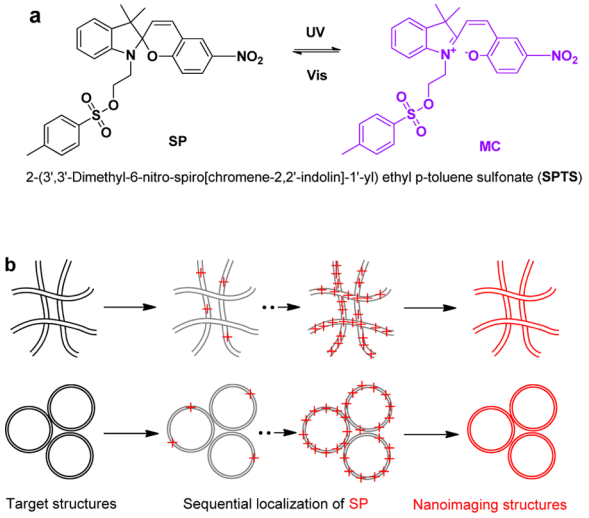

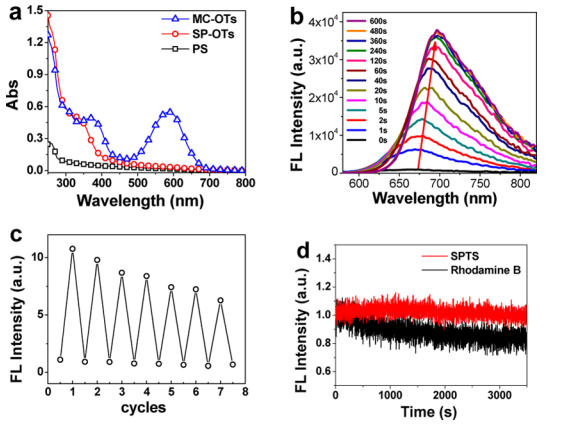

Figure 1. Optical properties of SPTS. (a) Absorption spectra of polystyrene (PSt), SPTS in PSt film before and after UV irradiation. (b) Emission spectra of SPTS in PSt film obtained at different time points during 365 nm UV irradiation. Excitation: 420 nm. (c) Switching curves of SPTS in PSt film. Excitation: 420 nm. (d) Photobleaching: SPTS and Rhodamine B in a PSt film were excited at 405 nm (SPTS kept in ON-states by continuous excitation at 405 nm). The fluorescent spectra of Rhodamine B are shown in Figure S1 of the Supporting Information.

by combining fluorescence microscopy techniques with photoswitchable fluorophores, one can probe a large field enough to be representative of the macroscopic sample and still preserve nanoscale information that is intrinsically encoded in the photoswitchable fluorescence signal.

The photoisomerization between SP and MC in hydrophobic polymer medium is induced by alternating UV−vis illumination (Scheme 1a). The coiled macromolecule chains in a good solvent become condensed in water, which allows for the segregation of hydrophobic SPs and hydrophobic polymer blocks from water (Scheme 1b). The self-assembly of block copolymers integrating hydrophobic SPs produces water-dispersible block copolymer micelles, including cylindrical micelles or polymer vesicles, which depend on the conditions of solution self-assembly. These microphase structures become emissive at UV irradiation followed by nonemissive at visible light illumination. On the basis of fluorescent switching of SPs, the microphase structures that are labeled with photoswitchable SPs become clear-cut with resolution beyond the optical diffraction limitation after algorithmic processing.

First we measured the optical absorption, emission, and fluorescence switching properties of SPTS in polystyrene (PSt) film, the staining agent used in optical nanoimaging of block copolymer self-assembly. As shown in Figure 1, panels a and b, UV-induced maximum absorption and emission wavelengths of SPTS in PSt film are about 590 and 690 nm, respectively. The color of SPTS-containing PSt colorless film quickly changes to purple upon exposure to UV irradiation at 365 nm for 5−10 s accompanied with the appearance of an absorption band at 590 nm. Incorporation of SPTS into the hydrophobic PSt medium could give rise to distinct on- and off-state fluorescence characteristics with pronounced sensitivity toward light. Upon UV light irradiation at 365 nm, the SPTS in PSt film are switched to the MC form in 5−10 s, and the fluorescence appears strong in deep red region at 670−690 nm (Figure 1b). In the reverse process, the red emission at 690 nm from MC form disappears after about 60−120 min of visible light illumination (Figure S2, Supporting Information). The reversible fluorescence of the SPTS in PSt film is repetitively highlighted with alternating UV ($\lambda < 420$ nm) and visible ($\lambda > 420$ nm) light irradiation. As shown in Figure 1, panel c, fluorescence switching of SPTS with UV and visible light is reversible in fluorescent intensity at least for seven cycles, with a little decay, though. The fluorescence at 690 nm is rapidly switched on upon 300−410 nm of UV irradiation. Similarly, visible light illumination above 500 nm causes gradient quenching of fluorescence at 690 nm. Our previous studies have also shown that the MC (open form of SP) incorporated into the hydrophobic core of polymer nanoparticles was highly luminescent.[25] In addition, the emission intensity of SPTS in open form at 405 nm excitation does not show noticeable decay compared with conventional Rhodamine B (Figure 1d). Consequently, SPTS could be used as staining agents for optical nanoimaging when SPTS is disposed in hydrophobic polymer medium.

A proof-of-principle system is realized by integrating the SPTS in self-assembly of block copolymer PSt-*b*-PEO ($M_{n,PSt}$ = 38 k, $M_{n,PEO}$ = 11 k). PSt-*b*-PEO block copolymer is composed of hydrophobic PSt block and a hydrophilic PEO block, in which PEO is covalently attached to PSt chain end. We use the reported approach for the formation of amphiphilic block copolymer micelles.[30] Fluorescence microscopic images with optical nanoimaging facility reveal that PSt-*b*-PEO self-assembles into cylindrical micelles in final aqueous dispersion. Optical images of the identical selected area are provided both in bright field mode to collect all transmitted light and fluorescence mode (561 nm excitation laser, 590 nm long pass filter) to collect only the fluorescence emitted by SPTS (Figure 2). The bright field image of cylindrical micelles shown in Figure 2, panel a indicates that the light scattering from PSt-*b*-PEO cylindrical micelles enables the preliminary optical observation of nanostructures. The image generated by fluorescent mode (Figure 2b) displays the corresponding landscapes to the image in transmitted mode (Figure 2c). The bright field and fluorescence image indicate that the mean diameter of cylindrical is almost 1 μm and 300−400 nm, respectively. However, the real diameter of cylindrical micelles (usually tens of nanometers) is inaccessible because of optical limits of diffraction.

DOI: 10.1021/ja512189a
J. Am. Chem. Soc. 2015, 137, 2436−2439

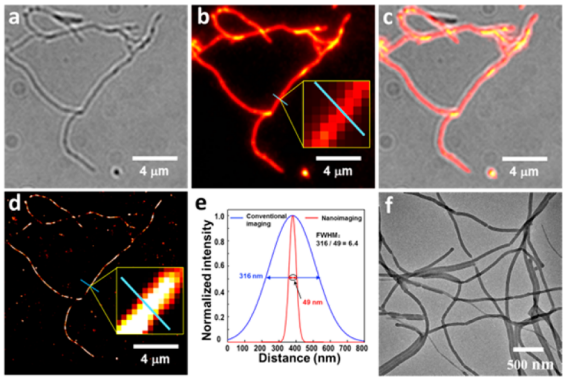

Figure 2. Optical nanoimaging of cylindrical micelles formed from PSt-*b*-PEO block copolymer self-assembly staining by photoswitchable SPTS. (a) Bright field image. (b) Conventional fluorescence image. Inset: high-magnification image, and each pixel size is 160 nm. (c) Merged bright field and fluorescence image. (d) Optical nanoimage corresponding to the same field of fluorescence image. Inset: high-magnification image, and each pixel size is 16 nm. (e) Fluorescence cross-sectional profiles of single cylindrical micelle and (f) TEM images of cylindrical micelles.

Photoswitchable SPTS is the solution to this issue. SPTS in hydrophobic polystyrene phase exhibits fluorescence switching upon alternating UV−vis irradiation. The optical properties of SP in cylindrical micelles are measured, which are similar to those in polystyrene film (Figure S3, Supporting Information). Thus, the SPTS-staining nanostructures can be reversibly highlighted using UV−vis excitation, which enables optical nanoimaging of staining nanostructures. The conventional fluorescence image and optical nanoimaging match exactly to bright field image of PSt-*b*-PEO cylindrical micelles. The clearer cylindrical microphase structure is observed in optical nanoimage (Figure 2d). The full-width at half-maximum (fwhm) of the localized single fluorescent micelle in Figure 2, panel d is determined from Gaussian deconvolution as low as to 49 nm, which is over six-times enhancement (Figure 2e). The overall resolution of the diffraction-unlimited image is calculated to be 38.6 ± 0.4 nm using the Fourier ring correlation[31] (Figure S4). The dimensional analysis of optical nanoimaging yields a diameter distribution of 66.5 ± 9.8 nm (Figure S5) and a length throughout from tens to hundreds of microns. Other optical nanoimages have also been provided in Figure S6. This indicates that optical nanoimaging can promote the optical resolution to tens of nanometers, which positively breaks optical diffraction limitation of conventional fluorescence imaging. The cylindrical micelles have also been identified by TEM and SEM (Figure 2f and Figure S5). The SEM and TEM images show that the relative low contents of SPTS do not affect the shapes of block copolymer micelles (Figure S7 and S8). The diameter distributions of cylindrical micelles are 55.6 ± 4.3 nm and 61.2 ± 7.2 nm for TEM and SEM, respectively (Figure S5). The comparable morphological observation and quantitative size measurement of micelles in optical nanoimaging, SEM, and TEM indicate that optical nanoimaging is a promising approach to characterize block copolymer microphase structures.

Monitoring real time dynamic process using optical nanoimaging is also desirable. Under fluorescent microscope, it is observed that PSt-*b*-PEO and SPTS-containing chloroform droplets in SDS aqueous solution cannot suffer the interfacial surface tension after a certain time and are disintegrated in 10 s at a critical point, which is difficult to monitor by optical nanoimaging (Figure S9). Instead, the intermediate structures are captured by optical nanoimaging during the formation of cylindrical micelles. At 3 h, small aggregates about 1 μm are observed around the big vesicles (Figure S10). After about 6.5 h, the cylindrical micelles bud from the aggregates (Figure S11). The conventional optical image is fuzzy, and the nearby micelles cannot be distinguished. Until 12 h after the emulsion is exposed to the atmosphere, the uniform cylindrical micelles are observed (Figure S12). Although in situ optical nanoimaging in real time is not achieved so far, we believed that the improvement of optical hardware and software as well as the probes will make it possible in the future.

It is essential to underscore significant morphological differences in microphase structures for a given PSt-*b*-PEO diblock copolymer self-assembly under different conditions. We have found that the block copolymer vesicles in aqueous solution, named as polymersomes, are also produced by using the same method when the concentration of SDS aqueous solution is decreased.[30] The morphological transition from cylindrical micelles to polymersomes can be observed in SEM (Figures S13 and S14). The polymersomes in solution were observed by fluorescence microscopy, optical nanoimaging, SEM, and TEM, which allowed for direct visualization and quantitative comparison of the aggregate microphase structures formed in aqueous suspension (Figure 3).

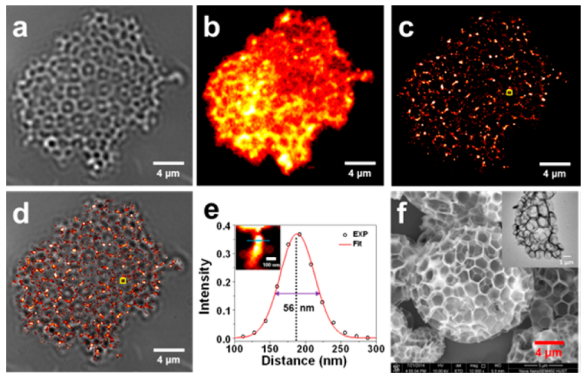

Figure 3. Optical nanoimaging of polymersomes formed from PSt-*b*-PEO block copolymer self-assembly stained by photoswitchable SPTS. (a) Bright field image. (b) Conventional fluorescence image. (c) Optical nanoimage corresponding to the same field of fluorescence image. (d) Merged bright field and optical nanoimage. (e) Fluorescence cross-sectional profiles of membrane bilayer of polymersomes. Inset: zoomed nanoimage from panels c and d. (f) SEM image of polymersomes. Inset: TEM image.

Figure 3, panel a shows bright field image of vesicle aggregates. The corresponding conventional fluorescence mode gives us a cloudy opaque image, which is difficult to obtain a clear contour of polymersomes (Figure 3b). The clearer microphase structure was observed in optical nanoimage (Figure 3c,d). The optical nanoimaging indicates that most of the fluorescence signals are dispersed in the hydrophobic bilayer walls of polymer vesicles. The discrete contour of polymer vesicles is observed, although continuous bilayer wall structures are not yet evident in optical nanoimaging. The fwhm of the continuous bilayer wall structures in Figure 3, panel d is determined from Gaussian deconvolution as low as to 56 nm (Figure 3e). Correspondingly, the result indicates that optical nanoimaging can promote the optical resolution to tens of nanometers. The aggregates of polymersomes are also observed in SEM and TEM (Figure 3f). Figure 3,

DOI: 10.1021/ja512189a
J. Am. Chem. Soc. 2015, 137, 2436−2439

panel f shows a 3D alveolate ball due to the collapse of polymersomes resulting from water evaporation in the vesicle aggregates. The TEM picture (inset) seems more comparable with the optical image.

In conclusion, we introduce an optical characterization approach named as optical nanoimaging toward microphase structures of block copolymer self-assembly in aqueous solution. The sub-100 nm microphase structures of block copolymer micelles have been conveniently observed in optical nanoimaging using SPTS as the staining agent. This represents an exploratory breakthrough in optical nanoimaging for block copolymer self-assembly, which has been more often characterized by SEM and TEM. By aid of suitable staining agents specific to different nanodomains or targets, it is promising to develop this optical nanoimaging as an innovative and universal optical characterization tool for multiphase polymers and composites with nanoscale resolution.

■ ASSOCIATED CONTENT

Supporting Information

Materials and methods. This material is available free of charge via the Internet at http://pubs.acs.org.

■ AUTHOR INFORMATION

Corresponding Author

*mqzhu@hust.edu.cn

Author Contributions

§J.Y., L.-X.Z., and C.L. contributed equally.

Notes

The authors declare no competing financial interest.

■ ACKNOWLEDGMENTS

This work was supported by the 973 Program of China (2015CB755602 and 2013CB922104), NSFC (21474034 and 21174045). We also thank the Analytical and Testing Center of Huazhong University of Science and Technology and the Center of Microfabrication and Characterization (CMFC) of WNLO for use of their facilities.

■ REFERENCES

(1) Bates, F. S.; Hillmyer, M. A.; Lodge, T. P.; Bates, C. M.; Delaney, K. T.; Fredrickson, G. H. *Science* **2012**, *336*, 434−440.

(2) Sai, H.; Tan, K. W.; Hur, K.; Asenath-Smith, E.; Hovden, R.; Jiang, Y.; Riccio, M.; Muller, D. A.; Elser, V.; Estroff, L. A.; Gruner, S. M.; Wiesner, U. *Science* **2013**, *341*, 530−534.

(3) Ruiz, R.; Kang, H.; Detcheverry, F. A.; Dobisz, E.; Kercher, D. S.; Albrecht, T. R.; de Pablo, J. J.; Nealey, P. F. *Science* **2008**, *321*, 936−939.

(4) (a) Liu, G.; Thomas, C. S.; Craig, G. S. W.; Nealey, P. F. *Adv. Funct. Mater.* **2010**, *20*, 1251−1257. (b) Liu, G.; Ramírez-Hernández, A.; Yoshida, H.; Nygård, K.; Satapathy, D. K.; Bunk, O.; Pablo, J. J.; de Nealey, P. F. *Phys. Rev. Lett.* **2012**, *108*, 065502. (c) Tavakkoli, A.; Gotrik, K. G.; K, W.; Hannon, A. F.; Alexander-Katz, A.; Ross, C. A.; Berggren, K. K. *Science* **2012**, *336*, 1294−1298.

(5) Geng, Y.; Discher, D. E. *J. Am. Chem. Soc.* **2005**, *127*, 12780−12781.

(6) Gaucher, G.; Dufresne, M. H.; Sant, V. P.; Kang, N.; Maysinger, D.; Leroux, J. C. *J. Controlled Release* **2005**, *109*, 169−188.

(7) Riess, G. *Prog. Polym. Sci.* **2003**, *28*, 1107−1170.

(8) (a) Wang, L.; Chen, D.; Sun, J. *Langmuir* **2009**, *25*, 7990−7994. (b) Wang, L.; Wang, X.; Xu, M.; Chen, D.; Sun, J. *Langmuir* **2008**, *24*, 1902−1909.

(9) Tao, W.; Liu, Y.; Jiang, B. B.; Yu, S. R.; Huang, W.; Zhou, Y. F.; Yan, D. Y. *J. Am. Chem. Soc.* **2012**, *134*, 762−765.

(10) (a) Zhou, X. Z.; Shade, C. M.; Schmucker, A. L.; Brown, K. A.; He, S.; Boey, F. Y. C.; Ma, J.; Zhang, H.; Mirkin, C. A. *Nano Lett.* **2012**, *12*, 4734−4737. (b) Lu, G.; Chen, Y.; Li, B.; Zhou, X.; Xue, C.; Ma, J.; Boey, F. Y. C.; Zhang, H. *J. Phys. Chem. C* **2009**, *113*, 4184−4187. (c) Li, H.; Wu, J.; Yin, Z.; Zhang, H. *Acc. Chem. Res.* **2014**, *47*, 1067−1075. (d) Lu, G.; Zhou, X.; Li, H.; Yin, Z.; Li, B.; Huang, L.; Boey, F.; Zhang, H. *Langmuir* **2010**, *26*, 6164−6166.

(11) (a) Xu, L.; Miao, X.; Ying, X.; Deng, W. *J. Phys. Chem. C* **2012**, *116*, 1061−1069. (b) Xu, L.; Miao, X.; Cha, B.; Deng, W. *J. Phys. Chem. C* **2012**, *116*, 16014−16022.

(12) (a) Wei, Z.; Gourevich, I.; Field, L.; Coombs, N.; Kumacheva, E. *Macromolecules* **2006**, *39*, 2441−2444. (b) Huang, B.; Bates, M.; Zhuang, X. *Annu. Rev. Biochem.* **2009**, *78*, 993−1016.

(13) (a) Ding, D.; Li, K.; Liu, B.; Tang, B. Z. *Acc. Chem. Res.* **2013**, *46*, 2441−2453. (b) Leung, C. W. T.; Hong, Y.; Chen, S.; Zhao, E.; Lam, J. W. Y.; Tang, B. Z. *J. Am. Chem. Soc.* **2013**, *135*, 62−65. (c) Chen, S.; Hong, Y.; Liu, Y.; Liu, J.; Leung, C. W. T.; Li, M.; Kwok, R. T. K.; Zhao, E.; Lam, J. W. Y.; Yu, Y.; Tang, B. Z. *J. Am. Chem. Soc.* **2013**, *135*, 4926−4929.

(14) Bates, M.; Huang, B.; Zhuang, X. *Curr. Opin. Chem. Biol.* **2008**, *12*, 505−514.

(15) (a) Hell, S. W.; Wichmann, J. *Opt. Lett.* **1994**, *19*, 780−782. (b) Ullal, C. K.; Schmidt, R.; Hell, S. W.; Egner, A. *Nano Lett.* **2009**, *9*, 2497−2500.

(16) Klar, T. A.; Hell, S. W. *Opt. Lett.* **1999**, *24*, 954−956.

(17) Gustafsson, M. G. L. *Proc. Natl. Acad. Sci. U.S.A.* **2005**, *102*, 13081−13086.

(18) Rust, M. J.; Bates, M.; Zhuang, X. *Nat. Methods* **2006**, *3*, 793−795.

(19) Bates, M.; Huang, B.; Dempsey, G. T.; Zhuang, X. *Science* **2007**, *317*, 1749−1753.

(20) Huang, B.; Wang, W.; Bates, M.; Zhuang, X. *Science* **2008**, *319*, 810−813.

(21) Huang, B.; Jones, S. A.; Brandenburg, B.; Zhuang, X. *Nat. Methods* **2008**, *5*, 1047−1052.

(22) Betzig, E.; Patterson, G. H.; Sougrat, R.; Lindwasser, O. W.; Olenych, S.; Bonifacino, J. S.; Davidson, M. W.; Lippincott-Schwartz, J.; Hess, H. F. *Science* **2006**, *313*, 1642−1645.

(23) Hess, S. T.; Girirajan, T. P. K.; Mason, M. D. *Biophys. J.* **2006**, *91*, 4258−4272.

(24) (a) Li, C.; Yan, H.; Zhang, G.-F.; Gong, W.-L.; Chen, T.; Hu, R.; Aldred, M. P.; Zhu, M.-Q. *Chem.—Asian J.* **2014**, *9*, 104−109. (b) Li, C.; Yan, H.; Zhao, L.-X.; Zhang, G.-F.; Hu, Z.; Huang, Z.-L.; Zhu, M.-Q. *Nat. Commun.* **2014**, *5*, 5709.

(25) (a) Zhu, M.-Q.; Zhang, G.-F.; Li, C.; Aldred, M. P.; Chang, E.; Drezek, R. A.; Li, A. D.-Q. *J. Am. Chem. Soc.* **2011**, *133*, 365−372. (b) Zhu, M.-Q.; Zhang, G.-F.; Li, C.; Li, Y.-J.; Aldred, M. P.; Li, A. D.-Q. *J. Innovative Opt. Health Sci.* **2011**, *4*, 395−408.

(26) (a) Zhu, M.-Q.; Zhu, L.; Han, J. J.; Wu, W.; Hurst, J. K.; Li, A. D. Q. *J. Am. Chem. Soc.* **2006**, *128*, 4303−4309. (b) Zhu, M.-Q.; Chen, T.; Zhang, G.-F.; Li, C.; Gong, W.-L.; Chen, Z.-Q.; Aldred, M. P. *Chem. Commun.* **2014**, *50*, 2664−2666.

(27) (a) Zhu, M.-Q.; Zhang, G.-F.; Hu, Z.; Aldred, M. P.; Li, C.; Gong, W.-L.; Chen, T.; Huang, Z.-L.; Liu, S. *Macromolecules* **2014**, *47*, 1543−1552. (b) Li, C.; Hu, Z.; Aldred, M.; Zhao, L.-X.; Yan, H.; Zhang, G.-F.; Huang, Z.-L.; Li, A.; Zhu, M.-Q. *Macromolecules* **2014**, *47*, 8594−8601.

(28) (a) Ullal, C. K.; Schmidt, R.; Hell, S. W.; Egner, A. *Nano Lett.* **2009**, *9*, 2497−2500. (b) Ullal, C. K.; Primpke, S.; Schmidt, R.; Böhm, U.; Egner, A.; Vana, P.; Hell, S. W. *Macromolecules* **2011**, *44*, 7508−7510. (c) Gramlich, M. W.; Bae, J.; Hayward, R. C.; Ross, J. L. *Opt. Express* **2014**, *22*, 8438−8450.

(29) (a) Dempsey, G. T.; Bates, M.; Kowtoniuk, W. E.; Liu, D. R.; Tsien, R. Y.; Zhuang, X. *J. Am. Chem. Soc.* **2009**, *131*, 18192. (b) Vaughan, J. C.; Dempsey, G. T.; Sun, E.; Zhuang, X. *J. Am. Chem. Soc.* **2013**, *135*, 1197−1200.

(30) (a) Zhu, J. T.; Hayward, R. C. *J. Am. Chem. Soc.* **2008**, *130*, 7496. (b) Zhu, J. T.; Ferrer, N.; Hayward, R. C. *Soft Matter* **2009**, *5*, 2471−2478.

(31) Nieuwenhuizen, R. P. J.; Lidke, K. A.; Bates, M.; Puig, D. L.; Grunwald, D.; Stallinga, S.; Rieger, B. *Nat. Methods* **2013**, *10*, 557−562.

DOI: 10.1021/ja512189a
J. Am. Chem. Soc. 2015, 137, 2436−2439